Photonic Crystal Selective Structures for Solar Thermophotovoltaics

Zhiguang Zhou[1], Enas Sakr[1], Omar Yehia[2], Anubha Mathur[1], and Peter Bermel[1]

[1] Purdue University, School of Electrical & Computer Engineering, 1205 W State St., West Lafayette, Indiana, USA, 47907

[2] Purdue University, School of Mechanical Engineering, 585 Purdue Mall, West Lafayette, Indiana, USA, 47907

ABSTRACT

Solar thermophotovoltaic (STPV) systems convert sunlight into electricity via thermal radiation. The efficiency of this process depends critically on both the selective absorber and the selective emitter, which are controlled by both the materials and the photonic design. For high concentration solar TPV applications, 2D photonic crystals (PhCs) made of refractory metals such as tungsten have demonstrated promising results. For even higher performance, we propose two photonic crystal-based designs to both collect solar heat and reradiate above-gap photons. First, a PhC selective structure (IPSS), which combines 2D photonic crystals and filters into a single device. Second, an Er-Yb-Tm co-doped fused silica coated with a 17-bilayer structure also offers significant selectivity with greater ease of fabrication. Finite difference time domain (FDTD) and rigorous coupled wave analysis (RCWA) simulations show that both can significantly suppress sub-bandgap photons. This increases sunlight-to-electricity conversion for photonic crystal-based emitters above 24.3% at 100 suns concentration or 27% at 1000 suns concentration using a $Ga_{0.42}In_{0.58}As$ PV diode with a bandgap of 0.7 eV (nearly lattice-matched to InP).

INTRODUCTION

Solar thermophotovoltaic (STPV) systems convert sunlight into electricity via thermal radiation. The efficiency of STPV depends on the product of the selective absorber thermal transfer efficiency[1] and the TPV system[2], which are controlled by both the materials and the photonic design. Metal-dielectric composites like cermets[3] and semiconductor-metal tandem[4] are strong candidates for operation of conditions such as 100 suns concentration and 1000 K. It is also demonstrated that with proper design and fabrication, single wall carbon nanotubes exhibit selective absorption as well[5]. For artificial photonic structures, plasmonic selective absorbers[6] were proposed to benefit from surface plasmon-enhanced absorption. Photonic crystals made of refractory metals[7] were also proposed to be highly efficient selective solar absorbers under high temperature (≥ 1000 K) and high concentrations (~ 1000 suns)[8–10]. Nevertheless, it can be more challenging to design a selective solar absorber at higher temperatures (~ 1500 K) and moderate solar concentrations (≤ 100 suns) for the highest performance and compatibility with the overall STPV system. One key challenge is that blackbody radiation at such high temperatures has strong overlap with the solar irradiance spectrum, making it extremely challenging to suppress thermal re-radiation while maintaining solar absorption. From a materials perspective, system integration may be facilitated by the use of similar materials and structures in both the selective solar absorber and the selective emitter. Given that the spectral requirement for selective solar absorbers and selective emitters are different[4], achieving this property together with the prior two can be even harder. To address the challenges discussed above, we propose two different selective solar absorber and emitter designs based on the selective emitter designs proposed in [11]. The first one is a rare earth based selective solar absorber, while the second one is an integrated photonic crystal absorber (IPSA).

For the first design, the naturally-sharp transitions of rare earth elements constitute a sharp cutoff for the solar absorber, and the cutoff wavelength will be governed by the longest wavelength transition of the rare earth dopant. Typically, rare earth ions are doped in host materials with sufficiently low absorption. Commonly used host materials are glasses and ceramics, especially for lasers, amplifier fibers, and thermal emitters[12,13]. We show that selecting the suitable dopants as well as a low-loss host material is the key to design an efficient solar absorber without the need to include filters on top of the structure. We propose two rare earth designs with chirped quarter-wave stack back reflectors suitable for operation under 100 suns and 1000 suns concentrations.

For the second design, the IPSA combines a 2D photonic crystal with a chirped rugate filter into a single device. By directly stacking the rugate filter on top of the 2D PhC, the sub-bandgap photon recycling[2] shifts to a non-perturbative regime instead of a perturbative one. The net effect is a strong selectivity in the absorbance spectrum. We show that when the proposed IPSA is combined with an integrated photonic crystal selective emitter (IPSE), the STPV conversion efficiency can be as high as 24.3%.

RARE EARTH BASED SELECTIVE SOLAR ABSORBER

Rare earth elements, such as Erbium, Thulium, Holmium and Ytterbium are known to have distinct atomic transitions identified in their absorption spectra. This property makes rare earths good candidates to provide sharp cut-off in the solar absorber spectrum. In designing a rare earth-based solar absorber, the selection of the host material, as well as the dopant element is crucial. First, dopants with atomic resonance wavelengths below the design cut-off wavelength should be selected. Among all rare earths, Erbium, Ytterbium, Thulium and Holmium exhibit absorption peaks, mostly in the visible and near infrared that makes them good candidates for dopant materials[14]. More specifically, co-doping of Er and Yb will show a cutoff wavelength at 1.65 µm, while co-doping Er, Yb, and Tm will show a cutoff wavelength at 1.9 µm. It is also important to increase the dopant concentration to maintain sufficient absorption for high energies using thick substrates, while keeping a minimal absorption at lower energies. Moreover, because the host material is naturally transparent, a back reflector is necessary for maximal absorption. A typical host material should exhibit sufficiently-low absorption over a wide range of wavelengths extending in the mid infrared. A promising candidate is fluoride glass, such as CaF_2 and BaF_2, with transmission bands between 0.16 µm and 10 µm, and base absorption coefficient as low as 7.8e-4 cm^{-1}, with a sufficiently-high melting point[15].

Two designs of solar absorbers are presented here, suited for 100 suns and 1000 suns, respectively. Both designs utilize a 17-bilayer chirped Bragg mirror of indices 2.3 and 1.48, which reflects over a broad range of absorbed wavelengths to reduce transmission losses. The first design is a thick Er-Yb-doped CaF_2 substrate of thickness 20 mm, reflective from 0.3 µm to 1.7 µm. The second design is an Er-Yb-Tm co-doped fused silica, of thickness 8 mm, with reflection extending from 0.3 µm to 2 µm. Emissivity spectra are calculated based on extracted material optical parameters for rare earth transitions from[16], and obtained using the simulation tool: "Thermophotonic selective emitter simulations," available on nanoHUB.org,[17] which simulates emissivity spectrum based on an open source rigorous coupled wave analysis (RCWA) simulation code [18] for multi-layer rare earth-based selective emitters/absorbers.

The emissivity spectra for both designs are depicted in figure 1, along with the AM1.5D solar spectrum. Since the rare earth-doped fused silica exhibits significant absorption starting at 4 µm, it will pose a limitation on the solar concentration requirement at 1500 K. Hence, greater

solar concentration is required to overcome the significant spectral overlap. Note also that neither Er nor Yb show absorption peaks at 1.2 µm – this gap reduces the maximum attainable thermal transfer efficiency. To assess the optimal operation conditions for the two given designs, a contour plot of the thermal transfer efficiency is shown for each design in Figure 2. Note that the thermal transfer efficiency is low in general with this design, since the coverage of the visible/near-IR spectrum is not complete, and due to significant emission past 7 µm. Higher efficiencies are obtained with the second design, as in Figure 2(b), for high concentrations and low temperatures. Finally, the STPV efficiency is computed for both designs, using a Sm-doped glass design of the emitter, similar to [11], assuming an ideal solar concentration efficiency. Figure 3(a) shows the STPV efficiency for the given designs. We note that for lower temperatures, the TPV conversion efficiency is low, while for higher temperatures, the thermal transfer efficiency is low, giving rise to an optimal efficiency point. For the first design under illumination of 100 suns, the optimal temperature is 1350 K with maximal efficiency of 12.9%. For the second design, under 1000 suns, the optimal temperature is 1500 K with maximal efficiency of 27%. A contour plot of the STPV efficiency for the Er-Yb-doped CaF_2 solar absorber is plotted in figure 3(b). The contour plot also shows a maximum efficiency of 19.1% achievable at 1650 K. The small remaining gaps in the visible/near-IR absorption spectrum could be addressed through further optimization of the dopant profiles and substrate thickness.

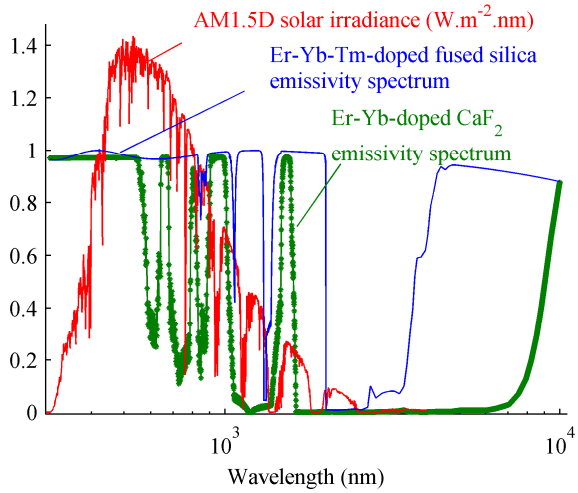

Figure 1 The emissivity spectrum of Er-Yb-Tm doped fused silica absorber (blue) and the emissivity spectrum of Er-Yb doped CaF_2 (green). The AM1.5D solar spectrum is plotted in red. Fused silica-based absorber shows IR absorption edge at 3.7 µm, while the CaF_2-based solar absorber shows extended flat minimal absorption band with an IR absorption edge at 7.5 µm that makes it a good candidate for low solar concentration (100 suns). The occupation of the spectrum also depends on the dopants, hence the cutoff for Er-Yb (green) is at 1.65 µm, while the cutoff of Er-Tm-Yb (blue) is at 1.9 µm.

Integrated Photonic Crystal Selective Structure

Another approach that is easier to engineer is photonic design. It has been shown that an integrated photonic crystal is strongly selective in its emittance spectrum[11]. Furthermore, its cut-off is in principle tunable with great flexibility. In order to achieve even higher STPV conversion efficiencies, we investigate an integrated photonic crystal structure (IPSS) that combines a selective absorber with a selective emitter as a single device.

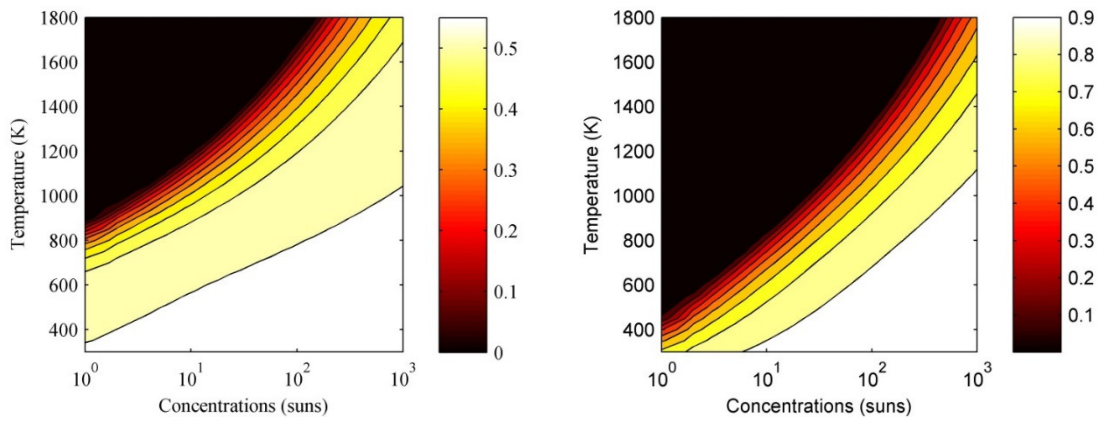

Figure 2. Contour plots of thermal transfer efficiency versus absorber temperature and solar concentration for (a) Er-Yb doped CaF_2, with high performance at 100 suns and 1500 K (b) Er-Yb-Tm doped fused silica with high efficiency at 1000 suns and 1500 K.

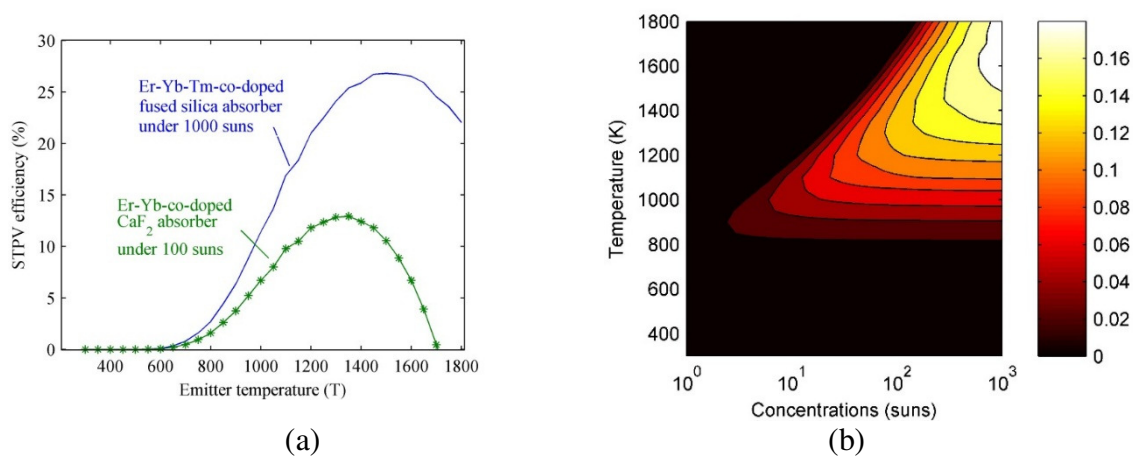

Figure 3. (a) STPV system efficiency, assuming a perfect solar concentration efficiency for two different slab absorber designs, combined with thermal emitter suggested in reference [11]. It is the product of thermal transfer efficiency and the TPV efficiency. Since the TPV efficiency decreases at lower temperature, and the thermal transfer efficiency decrease at higher temperatures, an optimal temperature is found for each design, which is 1350 K for the green curve and 1500 K for the blue curve. (b) A contour plot of the STPV efficiency for Er-Yb-based absorber, the maximum efficiency at 1000 suns is 19.1% at 1650 K.

The IPSS consists of an IPSA and IPSE. For the IPSA structure, the integrated filter is a piece of 60-period chirped rugate filter made of twenty materials with refractive indices ranging from $n_{SiO_2} = 1.46$ to $n_{SiO_2} = 2.50$. With the initial period thickness of 0.349 μm and a chirping

rate of 3.5%, the rugate filter has a broad stopband extending from 1.3 μm to 10 μm. Later, we will see that such broadband filtering allows the IPSA to have low (<10%) spectrally averaged absorbance[2] $\bar{\alpha}$ even at a temperature of 1500 K. The 2D PhC is made of tungsten (W) and has a square lattice with period $a = 0.470$ μm, hole radius $r = 0.293$ μm and hole depth $d = 2.386$ μm. Since the diameter of the holes are larger than the period, the PhC appears to be an array of W pillars, as schematically shown in figure 4(a). In order to integrate the filter with the 2D W PhC, spacing between the pillars are filled with the low index material SiO_2. For the IPSE, we choose the 15 bilayer integrated structure proposed in [11]. Both IPSA and IPSE have similar structural design and the 2D PhCs are both made of W. Therefore, when applied to an STPV system, the IPSA can be directly combined with the IPSE back to back as a single piece of IPSS absorber/emitter pair.

The absorbance spectrum of the designed IPSA is calculated using a finite difference time domain (FDTD)[19] method known as MEEP[20]. As shown in figure 4(b), the absorbance of IPSA has strong spectral selectivity near 1.3 μm. Beyond this cut-off, most of the thermal emission is suppressed. The enhanced absorbance below this cut-off covers the majority of the solar irradiance, yielding a spectrally averaged absorbance $\bar{\alpha} = 0.7686$. The absorbance spectrum of the IPSA is calculated up to 7 μm; the broad stopband of the rugate filter should make the absorbance negligible from this point to 10 μm. Thus, there is a numerical error no greater than 2.9% in the absorbance calculation due to the finite resolution and time for the region past 4 μm. At a temperature of 1500 K for example, the IPSA has a spectrally averaged emittance[2] $\bar{\varepsilon} = 0.0415$. The thermal transfer efficiency η_t at 100 suns solar concentration is then 65.0%, which is 6.9% below the maximum thermal transfer efficiency of 71.9% in the same condition (100 suns, 1500 K). In order to understand the performance of the proposed IPSA structure at various temperatures and solar concentrations, a contour plot of thermal transfer efficiency η_t as a function of temperature and solar concentration, as shown in figure 5(a), is calculated. It is obvious that η_t of the IPSA follows the same trend as the rare earth doped glass though the performance is better overall. The variation of η_t with solar concentration at high temperatures (> 1000 K) is smaller as well, due to the strongly selective absorbance of the IPSA. This offers the opportunity to achieve good STPV performance at low solar concentrations (≤ 100 suns), where only single axis precision tracking[21] is needed for highly efficient solar concentration, greatly reducing the system complexity. For a given solar concentration, higher temperature increases η_t while decreasing TPV conversion efficiency η_{tpv}. Such an intrinsic trade-off between η_t and η_{tpv} requires the investigation of the IPSS as a whole. Therefore, we calculate a contour plot of STPV conversion efficiency η_{stpv} for the IPSS as a function of temperature and solar concentration, neglecting concentration losses. The value of η_{tpv} at various temperatures for a PV diode with a bandgap of 0.7 eV ($Ga_{0.42}In_{0.58}As$) is calculated using current transport simulations available on nanoHUB.org[22]. As shown in figure 5(b), for each given solar concentration, an optimal temperature can be found. For the proposed IPSS structure under 100 suns concentration, the optimal temperature is 1450 K, where the IPSA has $\bar{\varepsilon} = 0.0354$ and $\eta_t = 68.0\%$. Assuming that the IPSE is at the same temperature as the IPSA in equilibrium, then $\eta_{tpv} = 35.7\%$, yielding $\eta_{stpv} = 24.3\%$.

CONCLUSIONS

We proposed two high-efficiency solar absorbers and emitters suitable for operation under 100 to 1000 suns concentrations for temperatures as high as 1500 K. Through careful selection of

materials or proper integrated photonic structure designs, high STPV conversion efficiencies can be achieved. We report a theoretical STPV efficiency of 24.3% under 100 suns and 1450 K using the IPSE design, and 12.93% at 1350 K and 100 suns using a rare earth-based solar absorber design. Under 1000 suns illumination, the latter design sees an optimal temperature of 1500 K with maximal efficiency of 27%. While the IPSS has much higher performance, the rare earth based absorber/emitter has a simpler structure for ease of fabrication. Further investigations on the rare earth based absorbers and the IPSS are warranted, including performance optimization and structural simplification.

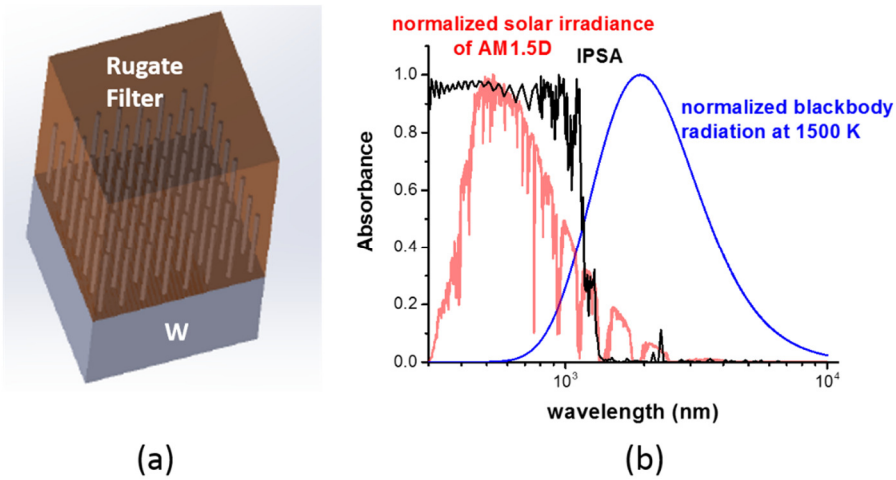

Figure 4. (a) Schematics of the IPSA structure; (b) Absorbance spectrum of the IPSA (black) plotted together with the normalized AM1.5D solar irradiance (red) and the normalized blackbody radiation at 1500 K (blue). The steep cut-off at 1.3 μm allows strong absorption of most solar irradiance while keeping the thermal emission low.

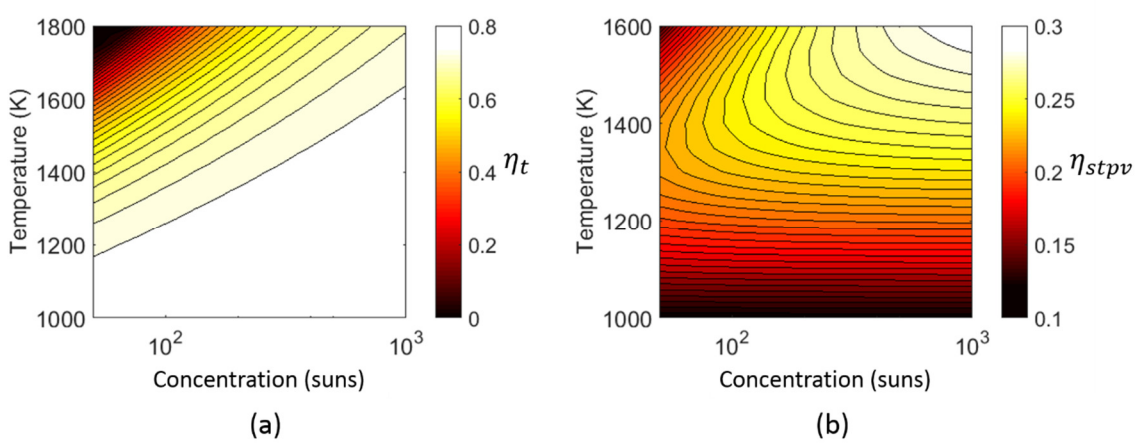

Figure 5. (a) Thermal transfer efficiency η_t as a function of temperature and solar concentration. For IPSA, the variation of η_t with concentrations at a given temperature is smaller compared with rare earth doped glass, making it possible for low concentration STPV applications. (b) STPV conversion efficiency as a function of temperature and solar concentration. For a given concentration of 100 suns, the optimal temperature is 1450 K, yielding $\eta_{stpv} = 24.3\%$.

ACKNOWLEDGMENTS

The authors thank Myles Steiner, Sasha Boltasseva, and Urcan Guler for valuable discussions. Support was provided by the Department of Energy, under DOE Cooperative Agreement No. DEEE0004946 (PVMI Bay Area PV Consortium), and the NSF Award EEC 1454315 - CAREER: Thermophotonics for Efficient Harvesting of Waste Heat as Electricity.

REFERENCES

[1] Q.-C. Zhang, J. Phys. D. Appl. Phys. **32**, 1938 (1999).
[2] P. Bermel, W. Chan, Y.X. Yeng, J.D. Joannopoulos, M. Soljacic, and I. Celanovic, in *TPV9 Ninth World Conf. Thermophotovoltaic Gener. Electr.* (2010).
[3] C.E. Kennedy, Thechnical Rep. NREL **CP02.2000**, 1 (2002).
[4] P. Bermel, M. Ghebrebrhan, W. Chan, Y.X. Yeng, M. Araghchini, R. Hamam, C.H. Marton, K.F. Jensen, M. Soljačić, J.D. Joannopoulos, S.G. Johnson, and I. Celanovic, Opt. Express **18 Suppl 3**, A314 (2010).
[5] T. Abendroth, H. Althues, G. Mäder, P. Härtel, S. Kaskel, and E. Beyer, *Sol. Energy Mater. Sol. Cells* **143**, 553 (2015).
[6] J. Liu, U. Guler, W. Li, A. Kildishev, A. Boltasseva, and V.M. Shalaev, in *CLEO* (2014), p. FM4C.5.
[7] Z. Zhou, Q. Chen, and P. Bermel, *Energy Convers. Manag.* **97**, 63 (2015).
[8] N.P. Sergeant, M. Agrawal, and P. Peumans, *Opt. Express* **18**, 5525 (2010).
[9] V. Rinnerbauer, A. Lenert, D.M. Bierman, Y.X. Yeng, W.R. Chan, R.D. Geil, J.J. Senkevich, J.D. Joannopoulos, E.N. Wang, M. Soljačić, and I. Celanovic, *Adv. Energy Mater.* **4** (2014).
[10] V. Rinnerbauer, E. Lausecker, F. Schäffler, P. Reininger, G. Strasser, and R.D. Geil, *Optica* **2**, 18 (2015).
[11] E. Sakr, Z. Zhou, and P. Bermel, in *SPIE Opt. Eng. + Appl.*, edited by M. Strojnik Scholl and G. Páez (International Society for Optics and Photonics, 2015), p. 960819.
[12] L. Huang, A. Jha, S. Shen, and X. Liu, *Opt. Express* **12**, 2429 (2004).
[13] R.A. Lowe, D.L. Chubb, S.C. Farmer, and B.S. Good, *Appl. Phys. Lett.* **64**, 3551 (1994).
[14] V.A.G. Rivera, E. Marega Jr, and F.A. Ferri. *Localized Surface Plasmon Resonances: Noble Metal Nanoparticle Interaction with Rare earth Ions*. Edited by K.Y. Kim (InTech, 2012).
[15] J.D. Traylor Kruschwitz and W.T. Pawlewicz, *Appl. Opt.* **36**, 2157 (1997).
[16] T. Schweizer, Rare earth-Doped Gallium Lanthanum Sulphide Glasses for Mid-Infrared Fibre Lasers, Optoelectronics Research Centre, University of Southampton and Institut für Laser-Physik, Universität Hamburg, 1998.
[17] A. Mathur, E. Sakr, P. Bermel "Thermophotonic Selective Emitter Simulation," DOI: 10.4231/D3S17ST4G. (2015).
[18] V. Liu and S. Fan, *Comput. Phys. Commun.* **183**, 2233 (2012).
[19] A. Taflove and S.C. Hagness, *Computational Electrodynamics: The Finite-Difference Time-Domain Method* (Artech House, 2000).
[20] A.F. Oskooi, D. Roundy, M. Ibanescu, P. Bermel, J.D. Joannopoulos, and S.G. Johnson, *Comput. Phys. Commun.* **181**, 687 (2010).
[21] H. Mousazadeh, A. Keyhani, A. Javadi, H. Mobli, K. Abrinia, and A. Sharifi, *Renew. Sustain. Energy Rev.* **13**, 1800 (2009).
[22] E. Schlenker, Z. Zhou, and P. Bermel, "Thermophotovoltaic Experiment," DOI: 10.4231/D3MW28G1H. (2015).